ONLINE METHODS

Cells, antibodies and reagents. HEK293T, A549 and HeLa cells were from American Type Culture Collection. MRC-5 (RCB0218) cells were provided by the RIKEN BioResource Center through the National Bio-Resource Project of the MEXT, Japan. All cells were cultured as described[54]. Peripheral blood mononuclear cells were isolated from peripheral venous blood of healthy volunteers (provided by the Hokkaido Red Cross Blood Center) by density-gradient centrifugation. Human primary $CD14^+$ monocytes (>95% $CD14^+$ as determined by flow cytometry) were obtained from peripheral blood mononuclear cells by magnetic-activated cell sorting with magnetic microbeads according to the manufacturer's instructions (Miltenyi Biotec). Experiments involving human blood were approved by the institutional review board of Hokkaido University. Antibodies used were as follows: anti-Flag (M2; Sigma), anti-hemagglutinin (5D8; MBL), antibody to green fluorescent protein (632375; Clontech), anti-RIG-I (8048849; ENZO Life Acience), anti-IRF3 (IRF3S1218-2; MBR), anti-ZCCHV (ab73369; Abcam), antibody to IFN-α/β receptor 2 (MMHAR-2; PBL) and anti-β-actin (AC-15; Sigma). The 3pRNA was prepared as reported[55]. Poly(dA:dT), poly(rI:rC), R-848 and human IFN-α were from Sigma, GE Healthcare, Alexis and Pepro Tech, respectively. Lipofectamine 2000 (Invitrogen) was used for transfection of nucleic acid ligands into the cytoplasm.

Plasmids and gene transfer. The cDNA for mouse PARP-1, PARP-2, PARP-7 (encoded by *Tiparp*), PARP-9, PARP-12 and PARP-13 (encoded by *Zc3hav1*), isoform 1 (ZAP) and isoform 2 (ZAPS) of human PARP-13 (encoded by *ZC3HAV1*), MAVS, RIG-I and the related mutants of ZAPS and RIG-I was obtained by RT-PCR of total RNA from mouse embryonic fibroblasts or HEK293T cells, then the cDNA was cloned into a pTA2 vector with the Target Clone-Plus-TA cloning kit (Toyobo). For YFP-, Flag- and HA-tagged proteins, cDNA was cloned into the XhoI and NotI sites of the pCAGGS-YFP, pCXN2-CFP, pCXN2-Flag or pIRM-3HA vector. The TLR8 expression vector was from Invivogen. The nucleotide sequence of each cDNA was confirmed with the BigDye Terminator v3.1 sequencing kit (Applied Biosystems). The vectors pCAGGS and Venus (called 'YFP' here) were provided by J. Miyazaki and A. Miyawaki, respectively. For the generation of expression plasmids for recombinant proteins, cDNA for ZAPS and ZAPSΔzf was cloned into the EcoRI and NotI sites of the pGEX-6P-1 (GE Healthcare), and cDNA for RIG-I was cloned into the SalI and NotI sites of pGEX-4T-3 (GE Healthcare). FuGENE6 (Roche) reagent was used for gene transfer with lipid transfection.

Quantitative RT-PCR analysis. Total RNA was analyzed by quantitative RT-PCR with the appropriate primers (sequences, **Supplementary Table 1**) and the ReverTra Ace Moloney murine leukemia virus reverse transcriptase with point mutations (Toyobo), SYBR Premix Ex Taq reagent mixture (TAKARA) and a StepOnePlus real-time PCR system (Applied Biosystems). Data were normalized to the expression of *ACTB* or *GAPDH* for each sample.

RNA-mediated interference. Chemically synthesized 21-nucleotide siRNA, including control siRNA (siPerfect Negative control), was obtained from Sigma (sequences, **Supplementary Table 2**). Cells were transfected with 50 nM siRNA in 2.0 μl Lipofectamine 2000 or Lipofectamine RNAiMAX (Invitrogen), then were used for further experiments 48 h later.

Reporter analysis. HEK293T cells seeded on 24-well plates were transiently cotransfected with luciferase reporter plasmids (100 ng each of pNF-κB-Luc (Clontech), p-55C1BLuc and p-125Luc (provided by T. Fujita)), together with increasing doses of expression vector or control vector. As an internal control, 10 ng renilla luciferase reporter plasmid was transfected simultaneously. Then, 48 h after transfection, cells were stimulated with 3pRNA or R-848 and luciferase activity was measured with the Dual-Luciferase Reporter Assay system (Promega).

Immunoblot analysis, immunoprecipitation assay and ELISA. Cell lysis, immunoblot analysis and immunoprecipitation assays were done as described[54]. Dimerization and oligomerization of IRF3 or RIG-I were assessed by native PAGE followed by immunoblot analysis as described[13,42,54]. IFN-β protein in culture supernatants was measured by ELISA according to the manufacturer's protocol (PBL).

Electrophoretic mobility-shift assay. For each sample, the same amount of nuclear protein extract (40 μg) was incubated with ^{32}P-radiolabeled oligonucleotide probe containing a consensus NF-κB-binding sequence, followed by analysis as described[54].

Fluorescence analysis. The YFP-ZAPS and Flag-tagged RIG-I expression vectors were transfected into HeLa cells at a concentration of 1.0 μg per well. Flag-tagged RIG-I was stained with anti-Flag and the appropriate secondary antibody conjugated to Alexa Fluor 594 (Molecular Probes). The localization of RIG-I and ZAPS was visualized with a BX61 confocal microscope (Olympus). FRET analysis was done as described[54]. Filters included U-MCFPHQ excitation-emission filters (Olympus) for YFP and CFP images and the CFP/YFP-2X2M-A filter set (Semrock) for FRET analysis. As a dichroic mirror, a UMREF glass reflector (Semrock) was used. Corrected FRET ($FRET^C$) was calculated with the following equation: $FRET^C = FRET - 0.5835 \times CFP - 0.1139 \times YFP$, where FRET, YFP and CFP indicate fluorescence intensity acquired for the FRET, YFP and CFP channels, respectively, with background fluorescence intensity subtracted.

Purification of recombinant proteins and *in vitro* ATPase assay. Glutathione *S*-transferase–tagged ZAPS, ZAPSΔzf and RIG-I proteins were expressed in *E. coli* strain BL21 and were purified with glutathione–Sepharose 4B beads according to the manufacturer's instruction (GE Healthcare). ATPase activity was measured by phosphate-release assay with the GREEN phosphate assay reagent (Biomol). Purified RIG-I protein (0.5 μg) and the appropriate amount of ZAPS or ZAPSΔzf protein in ATPase reaction buffer (20 mM Tris-HCl, pH 8.0, 1.5 mM $MgCl_2$ and 1.5 mM DTT) were incubated for 15 min at 37 °C with 1 μg 3pRNA, then further incubated for 15 min at 37 °C with 5 nmol ATP. Phosphate was then measured according to the manufacturer's protocol (Biomol).

Viral infection and plaque-forming assay. Cells were infected for 1 h at 37 °C with influenza A virus (strain A/X-31 (H3N2)) at a multiplicity of infection of 1.0 or 0.1 in infection medium (serum-free MEM containing amino acids and trypsin). Mardin-Darby canine kidney cells were used for plaque-forming assays. A549 and HEK293T cells were infected with NDV (provided by H. Kida) at a concentration of 25 hemagglutinating units per 1×10^6 cells, as described[54].

Establishment of human *ZC3HAV1*-knockout cells. *ZC3HAV1*-knockout cells were generated by CompoZr knockout ZFN technology according to the manufacturer's instruction (Sigma)[46]. First, mRNA or vector encoding the appropriate ZFN protein was transfected into HEK293T cells with Lipofectamine 2000. Then, 3 d after transfection, cells were replated into 96-well plates by limiting dilution (0.5 cells per well). The resulting genetic alterations were assessed by PCR and sequencing or by immunoprecipitation and immunoblot analysis.

Statistical analysis. Differences between control and experimental groups were evaluated with the Student's *t*-test.

54. Takaoka, A. *et al.* DAI (DLM-1/ZBP1) is a cytosolic DNA sensor and an activator of innate immune response. *Nature* **448**, 501–505 (2007).
55. Takahasi, K. *et al.* Solution structures of cytosolic RNA sensor MDA5 and LGP2 C-terminal domains: identification of the RNA recognition loop in RIG-I-like receptors. *J. Biol. Chem.* **284**, 17465–17474 (2009).

Journal of Gastroenterology and Hepatology

JGHF

doi:10.1111/j.1440-1746.2010.06375.x

GASTROENTEROLOGY

Lafutidine prevents low-dose aspirin and loxoprofen induced gastric injury: A randomized, double-blinded, placebo controlled study

Mototsugu Kato,* Go Kamada,† Keiko Yamamoto,† Urara Nishida,† Aki Imai,† Takeshi Yoshida,† Shouko Ono,* Manabu Nakagawa,* Soichi Nakagawa,* Yuichi Shimizu† and Masahiro Asaka†

*Division of Endoscopy, Hokkaido University Hospital, and †Department of Gastroenterology, Hokkaido University Graduate School of Medicine, Sapporo, Japan

Key words
aspirin, erosion, gastric mucosal injury, gastric ulcer, nonsteroidal anti-inflammatory drugs.

Accepted for publication 23 April 2010.

Correspondence
Professor Mototsugu Kato, Division of Endoscopy, Hokkaido University Hospital, North 14, West 5, Kita-ku, Sapporo, Hokkaido, Japan. Email: m-kato@med.hokudai.ac.jp

Abstract

Background and Aim: The concomitant use of non-steroidal anti-inflammatory drugs is a risk factor for low-dose aspirin (LDA)-associated upper gastrointestinal toxicity. Lafutidine is an H2-receptor antagonist with gastroprotective activity, produced by acting on capsaicin-sensitive afferent neurons. To evaluate the preventive effect of lafutidine on gastric damage caused by LDA alone and by the combination of both LDA and loxoprofen, we conducted a clinical study using healthy volunteers.

Methods: A randomized, double-blinded, placebo-controlled, crossover study was carried out. Sixteen healthy volunteers without *Helicobacter pylori* infection were randomly assigned to two groups. Both groups received 81 mg of aspirin once daily for 14 days (on days 1 to 14) and 60 mg of loxoprofen three times daily for the last 7 days (on days 8 to 14). Placebo or 10 mg of lafutidine was administered twice daily for 14 days in each group. After a 2-week washout period, placebo and lafutidine were crossed over. Endoscopic findings of gastric mucosal damage were evaluated according to the modified Lanza score.

Results: The mean modified Lanza score was 2.19 ± 1.06 (SD) for aspirin plus placebo as compared with 0.50 ± 0.77 for aspirin plus lafutidine ($P < 0.001$), and 3.00 ± 1.56 for aspirin plus loxoprofen and placebo as compared with 1.25 ± 1.37 for aspirin plus loxoprofen and lafutidine ($P < 0.01$).

Conclusions: The addition of loxoprofen to LDA increases gastric mucosal damage. Standard-dose lafutidine significantly prevents gastric mucosal damage induced by LDA alone or LDA plus loxoprofen in *H. pylori*-negative volunteers. Larger controlled studies are needed to strengthen these findings.

Introduction

Low-dose aspirin is widely used to prevent cerebrovascular disease and ischemic heart disease because of its antiplatelet activity.[1,2] Non-steroidal anti-inflammatory drugs (NSAIDs) are often used for the management of chronic pain associated with diseases such as rheumatoid arthritis and osteoarthritis. Because the prevalence of these diseases is particularly high among elderly patients, a growing proportion of such patients are likely to receive low-dose aspirin in combination with other NSAIDs.

Aspirin and other NSAIDs inhibit cyclooxygenase-1 (COX-1) and reduce the production of prostaglandins, which protect the gastrointestinal mucosa, leading to gastric mucosal damage.[3,4] These drugs have also been reported to directly injure the gastric mucosa under acidic conditions.[5,6]

Proton-pump inhibitors (PPIs), high-dose histamine (H2)-receptor antagonists, and misoprostol have been shown to prevent NSAID-induced gastrointestinal ulcers.[7–15] Lafutidine is an H2-receptor antagonist that continuously suppresses gastric-acid secretion and protects the gastric mucosa by acting on capsaicin-sensitive afferent neurons. Experimental studies have shown that lafutidine inhibits gastric mucosal damage induced by aspirin or other NSAIDs.[16] Aspirin and NSAIDs have caused acute gastric mucosal lesions in gastric corpus in rats. Lafutidine dose-dependently and significantly has prevented the development of gastric lesions.[16]

We compared the potential protective effect of lafutidine with that of placebo on gastric mucosal damage induced by low-dose aspirin alone or in combination with the NSAID loxoprofen in healthy volunteers who were not infected with *Helicobacter pylori (H. pylori)*. The present study represents the first use of lafutidine in human subjects for the prevention of gastric erosions.

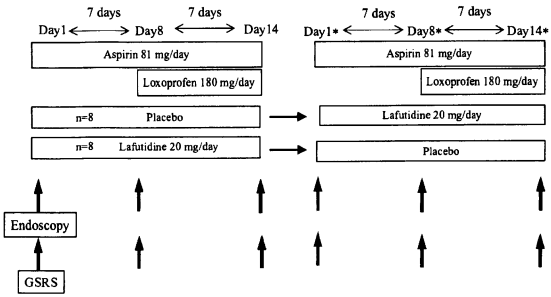

Figure 1 The design of the randomized, double-blinded, placebo-controlled, crossover study of endoscopic findings of gastric mucosal damage.

Methods

The study group comprised 16 healthy volunteers (13 men and three women) in whom *H. pylori* infection was negative on urea breath testing. They had no history of gastrointestinal ulcer, abdominal surgery, or *H. pylori* eradication therapy and had no disease currently being treated, bleeding gastrointestinal lesions, or drug allergy. Their mean age was 24.2 ± 2.0 (SD) years (range, 22 to 29). The study protocol was approved by the ethics committee of Hokkaido University School of Medicine. All patients gave written informed consent before study entry.

In the ^{13}C urea breath test, exhaled breath samples were collected in a specialized bag before and 20 min after oral administration of 100 mg of ^{13}C-urea (Otsuka Pharmaceutical Co., Ltd, Tokyo, Japan). Exhaled $^{13}CO_2$ was measured using an infrared spectrophotometer (UBiT-IR 300; Otsuka Pharmaceutical Co., Ltd, Tokyo, Japan).[17] The cut-off value for detecting *H. pylori* infection was defined as 2.5‰ at 20 min for the standard procedure.[18]

The study was conducted in a randomized, double-blinded, placebo-controlled, crossover fashion. The 16 volunteers were randomly assigned to group A (eight subjects) or group B (eight subjects). The subjects were not allowed to drink alcohol, smoke, or take other drugs from 1 week before the study until its completion (Fig. 1).

Group A received low-dose aspirin (Bristol-Myers K.K., Tokyo, Japan) in an oral dose of 81 mg once daily for 14 days (on days 1 to 14), loxoprofen (Daiichi-Sankyo Co., Ltd, Tokyo, Japan) in an oral dose of 60 mg three times daily for 7 days (on days 8 to 14), and lafutidine placebo, given orally twice daily for 14 days (on days 1 to 14).

Group B received low-dose aspirin and loxoprofen according to the same protocol as that described for group A. In addition, lafutidine (Taiho Pharmaceutical Co., Ltd, Tokyo, Japan) was given in an oral dose of 10 mg twice daily for 14 days (on days 1 to 14).

On day 0 (before receiving low-dose aspirin), day 7 (before receiving loxoprofen), and day 14 (after completing drug treatment), upper gastrointestinal endoscopy was performed, and symptoms were evaluated.

After a washout period of at least 2 weeks, the study treatment was crossed over, and group A and group B received the alternative treatment. To prevent gastric mucosal damage, rabeprazole (Eisai Co., Ltd, Tokyo, Japan) was given in a daily dose of 20 mg for the first 5 days of the washout period. On days 0, 7, and 14 after crossover of treatment (days 0*, 7*, and 14*), upper gastrointestinal endoscopy was carried out, and symptoms were evaluated.

Table 1 Criteria used to score gastric mucosal damage on endoscopic examination of three areas of the stomach: the antrum, corpus, and fornix

0: No lesions
1: One or two erosions or sites of mucosal hemorrhage in one gastric area
2: Three to five erosions or sites of mucosal hemorrhage in one gastric area
3: Five to 10 erosions or sites of mucosal hemorrhage in one gastric area or a few erosions or sites of mucosal hemorrhage in two gastric areas
4: More than 10 erosions throughout the stomach
5: Ulcer formation

Endoscopy was carried out six times (on days 0, 7, and 14 and days 0*, 7*, and 14*). Erosions, bleeding, and ulcers were assessed according to the modified Lanza score (Table 1, Fig. 2). Two endoscopists who were accredited members of the Japan Gastroenterological Endoscopy Society evaluated and scored the lesions. One endoscopist performed the endoscopic examinations and scored the lesions; the other endoscopist scored the lesions on the basis of the recorded endoscopic images. The mean values of these two evaluations were used as the final scores. Both endoscopists were blinded to treatment assignments.

Gastrointestinal symptoms were assessed according to the Japanese version of the Gastrointestinal Symptom Rating Scale (GSRS). The Japanese version of GSRS is a questionnaire that evaluates 15 items for five gastrointestinal symptoms (acid reflex, abdominal pain, dyspepsia, diarrhea, and constipation) according to a 7-grade scale. Before endoscopy, the subjects filled in the questionnaire six times, before each endoscopic examination.

Statistical analysis was carried out using StatMate III for Windows (ATMS Co., Ltd, Tokyo, Japan). Data were analyzed with the Mann–Whitney rank-sum test for patient demographics

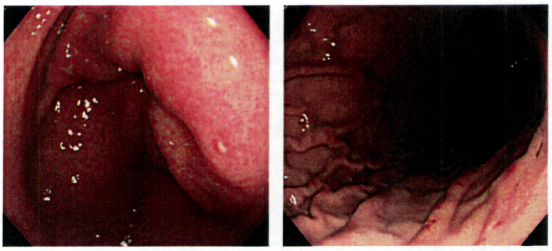

Figure 2 Endoscopic findings of gastric erosion and mucosal hemorrhage.

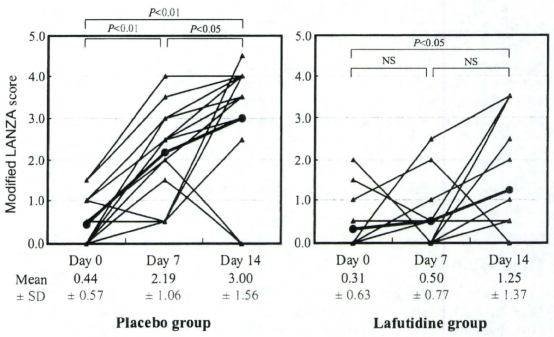

Figure 3 Comparison of changes in the modified Lanza score over time in each subject in the placebo group and the lafutidine group. The modified Lanza score increased significantly after use of low-dose aspirin only and concomitant use of low-dose aspirin and loxoprofen. —●—, 1–16 subjects; —■—, Mean ± SD.

and the Wilcoxon rank-sum test for Lanza score and GSRS data. *P*-values of less than 0.05 were considered to indicate statistical significance.

Results

Endoscopic findings (modified Lanza scores)

In the placebo group, the Lanza score significantly increased from 0.44 ± 0.57 (SD) (day 0) to 2.19 ± 1.06 (SD) (day 7) after 7 days of treatment with low-dose aspirin ($P < 0.01$). After concomitantly giving loxoprofen with low-dose aspirin for 7 days, the Lanza score increased significantly from 2.19 ± 1.06 (SD) (day 7) to 3.00 ± 1.56 (SD) (day 14) ($P < 0.05$). In the lafutidine group, the Lanza score did not increase significantly after 7 days of treatment with low-dose aspirin (day 0, 0.31 ± 0.63; day 7, 0.50). After adding loxoprofen to low-dose aspirin for 7 days, however, the Lanza score significantly increased from 0.50 ± 0.77 (SD) (day 7) to 1.25 ± 1.37 (SD) (day 14) (Fig. 3).

The mean modified Lanza score was 2.19 ± 1.06 (SD) for aspirin plus placebo as compared with 0.50 ± 0.77 (SD) for aspirin plus lafutidine ($P < 0.001$), and 3.00 ± 1.56 (SD) for aspirin plus loxoprofen and placebo as compared with 1.25 ± 1.37 (SD) for aspirin plus loxoprofen and lafutidine ($P < 0.01$) (Fig. 4).

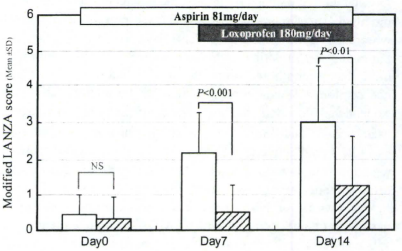

Figure 4 Comparison of the modified Lanza scores on days 0, 7, and 14 between the placebo group and the lafutidine group. The Lanza scores on days 7 and 14 were significantly lower in the lafutidine group than in the placebo group. □, Placebo; ▨, Lafutidine.

Gastrointestinal symptoms

The GSRS total scores on days 7 and 14 did not increase significantly as compared with the baseline values in either the placebo group or the lafutidine group. The GSRS total scores did not differ

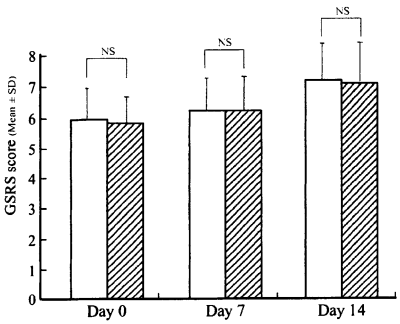

Figure 5 Comparison of the Gastrointestinal Symptom Rating Scale (GSRS) score on days 1, 7 and 14 between the placebo group and the laftideine group. There was no significant difference between the placebo group and the laftideine group. □, Placebo; ■, Lafutidine.

significantly between the placebo group and the lafutidine group on days 0, 7, or 14 (Fig. 5).

Discussion

The increasing incidence of cerebrovascular disease and ischemic heart disease has led to the increased use of low-dose aspirin. Gastrointestinal bleeding in patients receiving low-dose aspirin and other NSAIDs has become a problem. In the current study, gastric mucosal damage such as redness, petechia, and erosions (a modified Lanza score of 1 or higher) was present in all patients who received low-dose aspirin for 7 days. Yeomans *et al.* carried out endoscopy in patients who had received low-dose aspirin for more than 1 month and found that 10.7% had ulcers and 63.1% had erosions.[19] Nema *et al.* reported that the incidences of gastroduodenal ulcer and erosions were significantly higher in aspirin users (12.4% and 48.0%, respectively) than in non-users (7.3% and 12.2%, respectively).[20] Serrano *et al.* followed up 903 patients who received low-dose aspirin for 45 months on average and detected upper gastrointestinal bleeding in 41 (4.5%).[21]

Risk factors for NSAID-induced ulcers include a history of gastrointestinal ulcer, the use of NSAIDs, the concomitant use of anticoagulants and corticosteroids, advanced age, and cardiovascular disease.[22] In our study, the modified Lanza score increased by nearly twofold after concomitant use of low-dose aspirin and loxoprofen. Our study showed that adding an NSAID to low-dose aspirin exacerbated gastric mucosal damage. The incidence of aspirin-induced gastrointestinal bleeding has been reported not to differ according to the form or dose of aspirin.[22]

Proton-pump inhibitors, high-dose H_2-receptor antagonists, and misoprostol have been shown to prevent NSAID-induced ulcers.[7–15] PPIs and H_2-receptor antagonists act by suppressing gastric-acid secretion. Misoprostol protects the gastrointestinal mucosa by increasing prostaglandin production. Serrano *et al.* reported that PPIs and H_2-receptor antagonists decrease the risk of gastrointestinal bleeding by up to 22% in patients taking low-dose aspirin, as compared with non-users of these drugs.[21] Chan *et al.* compared the therapeutic usefulness of PPI with that of *H. pylori* eradication therapy in *H. pylori*-positive patients with a history of ulcer bleeding who were receiving low-dose aspirin or other NSAIDs. In patients given NSAIDs, PPI was more effective than eradication therapy for the prevention of recurrent bleeding. In low-dose aspirin users, however, there was no difference between PPI and eradication therapy.[23]

Several experimental studies have demonstrated that lafutidine inhibits gastric mucosal damage caused by aspirin or other NSAIDs.[16,24–28] In the current study, the Lanza scores on days 7 and 14 were significantly lower in the lafutidine group than in the placebo group. This finding suggested that lafutidine, given in the recommended dose for ulcers (20 mg/day), prevents gastric mucosal damage induced by low-dose aspirin alone or by combinations of low-dose aspirin and other NSAIDs. High doses of conventional H2-receptor antagonists have been reported to prevent NSAID-induced ulcers. However, our study showed lafutidine at the recommended dose for ulcers inhibited gastric mucosal damage associated with low-dose aspirin alone or with a combination of aspirin plus another NSAID. The mechanism of this effect is thought to involve the continuous suppression of gastric-acid secretion by lafutidine, as well as a protective effect on the gastric mucosa, mediated by the action of lafutidine on capsaicin-sensitive afferent neurons. Although the present study was carried out in *H. pylori*-negative, healthy volunteers, further clinical studies in patients receiving aspirin are needed to confirm our findings.

Patients who are receiving aspirin or other NSAIDs generally lack symptoms of gastrointestinal disturbances. Gastrointestinal bleeding is often detected on sudden episodes of hematemesis or melena.[29,30] There was no change in the symptom scores in our series, despite the presence of gastric mucosal damage on endoscopic examination.

In conclusion, a combination of low-dose aspirin and loxoprofen exacerbated gastric mucosal damage. As compared with placebo, lafutidine (20 mg/day) inhibited gastric mucosal damage induced by low-dose aspirin alone or a combination of low-dose aspirin and loxoprofen.

References

1 Antithrombotic Trialists' Collaboration. Collaborative meta-analysis of randomized trials of antiplatelet therapy for prevention of death, myocardial infarction, and stroke in high risk patients. *BMJ* 2002; **324**: 71–86.
2 Lauer MS. Aspirin for primary prevention of coronary events. *N. Engl. J. Med.* 2002; **346**: 1468–74.
3 Sakamoto C, Sugano K, Ota S *et al.* Case-control study on the association of upper gastrointestinal bleeding and nonsteroidal anti-inflammatory drugs in Japan. *Eur. J. Clin. Pharmacol.* 2006; **62**: 765–72.
4 Cryer B. Mucosal defense and repair. Role of prostaglandins in the stomach and duodenum. *Gastroenterol. Clin. North Am.* 2001; **30**: 877–94.
5 Davenport HW. Gastric mucosal injury by fatty and acetylsalicylic acids. *Gastroenterology* 1964; **46**: 245–53.
6 Sato Y, Asaka M, Takeda H, Ohtaki T, Miyazaki T. The

mechanisms of aspirin-induced gastric mucosal injury. *J. Clin. Gastroenterol.* 1993; **17** (Suppl. 1): S1–4.
7 Roth SH, Tindall EA, Jain AK *et al.* A controlled study comparing the effects of nabumetone, ibuprofen, and ibuprofen plus misoprostol on the upper gastrointestinal tract mucosa. *Arch. Intern. Med.* 1993; **153**: 2565–71.
8 Melo Gomes JA, Roth SH, Zeeh J, Bruyn GA, Woods EM, Geis GS. Double-blind comparison of efficacy and gastroduodenal safety of diclofenac/misoprostol, piroxicam, and naproxen in the treatment of osteoarthritis. *Ann. Rheum. Dis.* 1993; **52**: 881–5.
9 Graham DY, White RH, Moreland LW *et al.* Duodenal and gastric ulcer prevention with misoprostol in arthritis patients taking NSAIDs. Misoprostol Study Group. *Ann. Intern. Med.* 1993; **119**: 257–62.
10 Agrawal NM, Van Kerckhove HE, Erhardt LJ, Geis GS. Misoprostol coadministered with diclofenac for prevention of gastroduodenal ulcers. A one-year study. *Dig. Dis. Sci.* 1995; **40**: 1125–31.
11 Bocanegra TS, Weaver AL, Tindall EA *et al.* Diclofenac/misoprostol compared with diclofenac in the treatment of osteoarthritis of the knee or hip: a randomized, placebo controlled trial. Arthrotec Osteoarthritis Study Group. *J. Rheumatol.* 1998; **25**: 1602–11.
12 Taha AS, Hudson N, Hawkey CJ *et al.* Famotidine for the prevention of gastric and duodenal ulcers caused by nonsteroidal antiinflammatory drugs. *N. Engl. J. Med.* 1996; **334**: 1435–9.
13 Yeomans ND, Tulassay Z, Juhász L *et al.* A comparison of omeprazole with ranitidine for ulcers associated with nonsteroidal antiinflammatory drugs. Acid Suppression Trial: ranitidine versus omeprazole for NSAID-associated Ulcer Treatment (ASTRONAUT) Study Group. *N. Engl. J. Med.* 1998; **338**: 719–26.
14 Hawkey CJ, Karrasch JA, Szczepański L *et al.* Omeprazole compared with misoprostol for ulcers associated with nonsteroidal antiinflammatory drugs. Omeprazole versus Misoprostol for NSAID-induced Ulcer Management (OMNIUM) Study Group. *N. Engl. J. Med.* 1998; **338**: 727–34.
15 Bianchi Porro G, Lazzaroni M, Petrillo M, Manzionna G, Montrone F, Caruso I. Prevention of gastroduodenal damage with omeprazole in patients receiving continuous NSAIDs treatment. A double blind placebo controlled study. *Ital. J. Gastroenterol. Hepatol.* 1998; **30**: 43–7.
16 Tsuchiya S, Nakamura T, Yano S. Inhibitory effects of simultaneously applied lafutidine with NSAIDs on formation of gastric mucosal lesions in rats. *Jpn. Pharmacol. Ther.* 2007; **35**: 159–64.
17 Ohara S, Kato M, Asaka M, Toyota T, UBiT study Group. The UBiT-100 ^{13}CO2 infrared analyzer: comparison between infrared spectrometric analysis and mass spectrometric analysis. *Helicobacter* 1998; **3**: 49–53.
18 Ohara S, Kato M, Asaka M, Toyota T, C-13UBT Study Group. Studies of ^{13}C-urea breath test for diagnosis of *Helicobacter pylori* infection in Japan. *J. Gastroenterol.* 1998; **33**: 6–13.
19 Yeomans ND, Lanas AI, Talley NJ *et al.* Prevalence and incidence of gastroduodenal ulcers during treatment with vascular protective doses of aspirin. *Aliment. Pharmacol. Ther.* 2005; **22**: 795–801.
20 Nema H, Kato M, Asaka M *et al.* Investigation of gastric and duodenal mucosal defects caused by low-dose aspirin in patients with ischemic heart disease. *J. Clin. Gastroenterol.* 2009; **43**: 130–2.
21 Serrano P, Lanas A, Arroyo MT, Ferreira IJ. Risk of upper gastrointestinal bleeding in patients taking low-dose aspirin for the prevention of cardiovascular diseases. *Aliment. Pharmacol. Ther.* 2002; **16**: 1945–53.
22 Scheiman JM, Cryer B, Asaka M *et al.* Panel Discussion: treatment approaches to control gastrointestinal risk and balance cardiovascular risks and benefits: proposals and recommendations. *Aliment. Pharmacol. Ther. Symp. Ser.* 2005; **1**: 26–32.
23 Chan FK, Chung SC, Suen BY *et al.* Preventing recurrent upper gastrointestinal bleeding in patients with *Helicobacter pylori* infection who are taking low-dose aspirin or naproxen. *N. Engl. J. Med.* 2001; **344**: 967–73.
24 Ito H, Naito T, Takeyama M. Lafutidine changes levels of somatostatin, calcitonin gene-related peptide and secretin in human plasma. *Biol. Pharm. Bull.* 2002; **25**: 379–82.
25 Onodera S, Shibata M, Tanaka M *et al.* Gastroprotective activity of FRG-8813, a novel histamine H2-receptor antagonist, in rats. *Jpn. J. Pharmacol.* 1995; **68**: 161–73.
26 Sato H, Kawashima K, Yuki M *et al.* Lafutidine, a novel histamine H2-receptor antagonist, increases serum calcitonin gene-related peptide in rats after water immersion-restraint stress. *J. Lab. Clin. Med.* 2003; **141**: 102–5.
27 Ichikawa T, Ishihara K, Saigenji K, Hotta K. Lafutidine-induced stimulation of mucin biosynthesis mediated by nitric oxide is limited to the surface mucous cells of rat gastric oxyntic mucosa. *Life Sci.* 1998; **62**: PL259–64.
28 Ichikawa T, Ota H, Sugiyama A *et al.* Effects of a novel histamine H2-receptor antagonist, lafutidine, on the mucus barrier of human gastric mucosa. *J. Gastroenterol. Hepatol.* 2007; **22**: 1800–5.
29 Loeb DS, Talley NJ, Ahlquist DA, Carpenter HA, Zinsmeister AR. Long-term nonsteroidal anti-inflammatory drug use and gastroduodenal injury: the role of *Helicobacter pylori*. *Gastroenterology* 1992; **102**: 1899–905.
30 Katzka DA, Sunshine AG, Cohen S. The effect of nonsteroidal antiinflammatory drugs on upper gastrointestinal tract symptoms and mucosal integrity. *J. Clin. Gastroenterol.* 1987; **9**: 142–8.

DOI:10.1158/1078-0432.CCR-10-0548

Clinical Cancer Research

Imaging, Diagnosis, Prognosis

See commentary p. 3822

A Novel FRET-Based Biosensor for the Measurement of BCR-ABL Activity and Its Response to Drugs in Living Cells

Tatsuaki Mizutani[1], Takeshi Kondo[2], Stephanie Damanin[1,2], Masumi Tsuda[1], Shinya Tanaka[3], Minoru Tobiume[4], Masahiro Asaka[2], and Yusuke Ohba[1]

Abstract

Purpose: To develop a novel diagnostic method for the assessment of drug efficacy in chronic myeloid leukemia (CML) patients individually, we generated a biosensor that enables the evaluation of BCR-ABL kinase activity in living cells using the principle of fluorescence resonance energy transfer (FRET).

Experimental Design: To develop FRET-based biosensors, we used CrkL, the most characteristic substrate of BCR-ABL, and designed a protein in which CrkL is sandwiched between Venus, a variant of YFP, and enhanced cyan fluorescent protein, so that CrkL intramolecular binding of the SH2 domain to phosphorylated tyrosine (Y207) increases FRET efficiency. After evaluation of the properties of this biosensor by comparison with established methods including Western blotting and flow cytometry, BCR-ABL activity and its response to drugs were examined in CML patient cells.

Results: After optimization, we obtained a biosensor that possesses higher sensitivity than that of established techniques with respect to measuring BCR-ABL activity and its suppression by imatinib. Thanks to its high sensitivity, this biosensor accurately gauges BCR-ABL activity in relatively small cell numbers and can also detect <1% minor drug-resistant populations within heterogeneous ones. We also noticed that this method enabled us to predict future onset of drug resistance as well as to monitor the disease status during imatinib therapy, using patient cells.

Conclusion: In consideration of its quick and practical nature, this method is potentially a promising tool for the prediction of both current and future therapeutic responses in individual CML patients, which will be surely beneficial for both patients and clinicians. *Clin Cancer Res; 16(15); 3964–75. ©2010 AACR.*

The past few decades have witnessed considerable advances in our understanding of the molecular basis of pathophysiology underlying a wide range of diseases, including cancer. This knowledge has provided a platform for the development of molecular therapies aiming to specifically inhibit oncoproteins involved in signal transduction within tumor cells. This therapeutic concept has currently moved beyond the proof-of-concept stage; a substantial number of such inhibitors is successfully developed and presently in use against various cancers in the clinic, some of which have produced significant outcomes (1).

Chronic myeloid leukemia (CML) is a myeloproliferative disorder characterized by the presence of the Philadelphia chromosome (Ph), which is identifiable by cytogenetic analysis throughout the course of the disease (2). The Ph results from a reciprocal translocation between the long arms of chromosomes 9 and 22, t(9;22)(q34; q11), leading to the formation of a novel fusion gene, *Bcr-abl*. Because the subsequent chimeric BCR-ABL tyrosine kinase possesses constitutive activity and plays a critical role in the pathogenesis of CML (3, 4), it is not surprising that the introduction of imatinib mesylate (IM; previously known as STI571)—the first approved tyrosine kinase inhibitor—which functions by blocking the ATP binding site of BCR-ABL (5), has radically innovated the treatment of chronic phase CML (6). Patients with more advanced phases also respond to IM; but disappointingly, this occurs much less frequently and efficacy is less durable (7). Therefore, second-generation compounds, such as nilotinib (NL) and dasatinib (DS), are now available for the treatment of CML patients in whom IM treatment is ineffective (8). Similar newer agents,

Authors' Affiliations: [1]Laboratory of Pathophysiology and Signal Transduction, [2]Department of Gastroenterology and Hematology, and [3]Laboratory of Cancer Research, Hokkaido University Graduate School of Medicine, Sapporo, Japan; and [4]Department of Pathology, National Institute for Infectious Diseases, Tokyo, Japan

Note: Supplementary data for this article are available at Clinical Cancer Research Online (http://clincancerres.aacrjournals.org/).

T. Kondo and S. Damanin contributed equally to this work.

Corresponding Author: Yusuke Ohba, Laboratory of Pathophysiology and Signal Transduction, Hokkaido University Graduate School of Medicine, N15W7, Kita-ku, Sapporo 060-8638, Japan. Phone: 81-11-706-5158; Fax: 81-11-706-7877; E-mail: yohba@med.hokudai.ac.jp.

doi: 10.1158/1078-0432.CCR-10-0548

DOI:10.1158/1078-0432.CCR-10-0548

Translational Relevance

Imatinib, a drug targeting the oncogenic chimeric kinase BCR-ABL that is causatively expressed in chronic myeloid leukemia (CML) cells, is now frontline therapy for this disease because of its remarkable clinical activity. However, there is growing concern about the emergence of imatinib resistance, which supervenes, especially in advanced cases. The biosensor designed in this study cannot only accurately evaluate BCR-ABL activity in living CML cells and detect minor drug-resistant populations within heterogeneous ones but also enables the prediction of future onset of imatinib resistance and identification of the next therapeutic option for resistant cells, including dose escalation, combination therapy, and second generation inhibitors. Given the exclusive nature of our system, which reports BCR-ABL activity irrespective of the amount of protein present, as opposed to other conventional techniques, the addition of this novel prognostic indicator to the current CML therapeutic armamentarium is ultimately envisaged.

which are currently in clinical trials, might also be expected to enter the market in the very near future. As a favorable outcome in first-line therapy is critical for obtaining a better prognosis in CML patients (9), these rapid advances in treatment in turn warrant the development of techniques for evaluating drug efficacy in each individual patient, not only at the time of initial diagnosis but also during the course of the disease, thus increasing the likelihood of therapeutic success.

CrkL, a member of the Crk adaptor molecules, mediates a variety of pathophysiologic signaling involved in cell proliferation, differentiation, migration, and transformation (10). Like the other family member CrkII, it consists of one src homology (SH) 2 domain, two SH3 domains, and a tyrosine residue that is phosphorylated by cellular tyrosine kinases. In human CML cells, CrkL is identified as a major substrate of BCR-ABL and is constitutively phosphorylated, playing important roles in oncogenic signal transduction (11–13). As such, the level of CrkL phosphorylation, as analyzed by immunoblotting, has been used as a marker of BCR-ABL activity and drug responses (14). In this study, we develop an original system to determine BCR-ABL activity and its inhibition in response to drug treatment in living cells using the principle of fluorescence resonance energy transfer (FRET). The probe molecule constructed here measures BCR-ABL activity as changes in FRET efficiency, which facilitates the assessment of drug efficacy at a single cell level.

Materials and Methods

Plasmids, reagents, and antibodies

Details about the construction of plasmids are described in Supplementary Data. IM and NL were kind gifts from Novartis Pharma; DS was from Bristol-Myers Squibb. Anti-CrkL antibody (#3182; 1:1,000 dilution) and anti-phospho CrkL (Y207) antibody (#3181; 1:1,000 and 1:500 dilutions for immunoblotting and immunofluorescence, respectively) were purchased from Cell Signaling Technology, whereas anti–c-Abl antibody was obtained from Santa Cruz Biotechnology (sc-23; 1:500 and 1:100 dilutions).

Cell culture and transfection

293F cells were purchased from Invitrogen, maintained in Freestyle 293 expression medium (Invitrogen) or DMEM (Sigma-Aldrich) supplemented with 10% (v/v) fetal bovine serum, and transfected using 293fectin (Invitrogen) according to the manufacturer's protocol. The Ph-positive CML cell lines K562 and KU812 cells were obtained from Riken; HL60 and U937 were from the Japanese Collection of Research Bioresources cell bank. These four cell lines were maintained in RPMI 1640 (Sigma-Aldrich) supplemented with 10% (v/v) fetal bovine serum. Gene transfer into these cells was done using nucleofection according to the manufacturer's recommendations (Amaxa Biosystems)—~30% transfection efficacy was obtained for these leukemia cell lines.

Fluorescence spectrometry and immunoblotting

Cells were transfected with Pickles, with or without pCMV-3Myc-BCR-ABL. From 24 hours after transfection, a fluorescence spectrum was obtained by means of an FP-6500 fluorescence spectrometer (JASCO Co.), with an excitation wavelength of 420 nm. In some experiments, the cells were treated with IM (as indicated in the figure legends) before spectrometric analysis. To obtain the spectra of cell lysates, cells were harvested by centrifugation, lysed in lysis buffer [20 mmol/L Tris-HCl (pH 7.5), 100 mmol/L NaCl, 0.5% (NP40)], clarified by additional centrifugation, and subjected to spectroscopy. The same lysates were analyzed by immunoblotting as previously described (15).

Fluorescence microscopy

Cells expressing Pickles were cultured in phenol red-free RPMI 1640 (Invitrogen) buffered with 15 mmol/L HEPES (pH 7.4; to avoid CO_2 control), plated on a poly-L-lysine–coated glass base plate (Asahi Techno Glass Co.), and treated with indicated doses of IM, NL, and DS. Cell image acquisition was done as previously described (see also Supplementary Data; ref. 16). Following background subtraction, FRET/enhanced cyan fluorescent protein (ECFP) ratio images were created using MetaMorph software, and the images were used to illustrate FRET efficiency. In the dot plots, the absolute values for FRET/ECFP were calculated and plotted, one dot representing the FRET efficiency of a single cell.

Flow cytometry

Cells were fixed in 4% paraformaldehyde for 30 minutes at room temperature, permeabilized by saponin, and incubated with phospho-CrkL antibody (1:100 dilution). After

DOI:10.1158/1078-0432.CCR-10-0548

extensive washing, the cells were then incubated with Alexa Fluor 488–conjugated secondary antibody (1:500 dilution) and subjected to flow cytometric analysis using a FACSCalibur machine (Becton, Dickinson and Company) as previously described (17).

Clinical samples

This study was reviewed and approved by the Institutional Review Board of the Hokkaido University Graduate School of Medicine, and all patients provided informed consent before collection of bone marrow or peripheral blood samples. Bone marrow mononuclear cells (BMC) and peripheral blood mononuclear cells (PBMC) were isolated from bone marrow and peripheral blood samples using Lymphoprep (Nycomed), transfected with Pickles by nucleofection (Amaxa Biosystems; program number T-020 and Solution V), and maintained in RPMI supplemented with 10% fetal bovine serum. After 18 to 24 hours of transfection, the cells were treated with 2 μmol/L IM and then subjected to microscopic analysis to determine FRET efficiency (the transfection efficiency obtained was 20%).

Statistical analyses

All data, unless otherwise specified, are expressed as the mean ± SD, subjected to one-way ANOVA, and followed by comparison using a Student's or Welch's *t* test to evaluate the difference between the drug-treated and non-treated samples. Using either test, $P < 0.05$ was considered significant and is represented by an asterisk over the error bars in the figures. A threshold value, D-FRET, was introduced into the quantitative analyses to evaluate drug efficacy in heterogeneous cell populations. This value was defined by the following formula: D-FRET = average + (3 × SD) of the FRET efficiencies in 293F cells without BCR-ABL expression (= 2.04). Cells exhibiting FRET efficiency higher than D-FRET were designated as $FRET^{hi}$, whereas cells exhibiting FRET efficiency lower than D-FRET were called $FRET^{lo}$. Theoretically, 99.7% of 293F cells (without BCR-ABL expression) are expected to be $FRET^{lo}$ (18).

Results

Development of FRET-based probes to evaluate BCR-ABL activity

To develop FRET-based biosensors for monitoring BCR-ABL activity in living cells, we used CrkL, the most characteristic substrate of BCR-ABL (11–13), and designed a protein in which CrkL is sandwiched between Venus, a variant of YFP, and ECFP, so that CrkL intramolecular binding of the SH2 domain to phosphorylated tyrosine (Y207) increases FRET efficiency (Fig. 1A and B). This chimeric protein was named Pickles: phosphorylation indicator of CrkL *en* substrate. Despite the fact that it was efficiently phosphorylated, the prototype Pickles (Pickles-1.00) showed only a marginal difference in FRET efficiency in the presence of BCR-ABL (Supplementary Fig. S1A; Fig. 1C). Because the use of a truncated form of CrkII, a Crk family member highly homologous to CrkL, was previously reported to have improved the increase in FRET efficiency of a similar CrkII FRET-based probe (19), we substituted CrkL in Pickles-1.00 with a COOH terminus–truncated form (corresponding to amino acids 1-222) of CrkL (Fig. 1B). The FRET efficiency of Pickles-2.00 was significantly increased (by up to 30%) in the presence of BCR-ABL (Supplementary Fig. S1A; Fig. 1C).

To expand the dynamic range of Pickles-2.00, we introduced circular permutations, one of the rational methods to refine FRET probes (20), in ECFP (cpECFP), in which the NH_2- and COOH-terminal portions were interchanged and the original termini were reconnected by a short spacer (Fig. 1B). Among the several probes constructed, Pickles-2.30 exhibited the most significant increase in FRET efficiency (~40%) in the presence of BCR-ABL (Supplementary Fig. S1A; Fig. 1C). Furthermore, a study by Yoshizaki et al. (21) showed that the introduction of monomeric fluorescent proteins can improve the sensitivity of FRET-based probes, wherein the inhibition of fluorescent protein dimer/tetramer formation can possibly diminish false-positive FRET in the quiescent state (unphosphorylated Pickles in this case). Therefore, we substituted Venus in Pickles-2.30 with monomeric Venus-L222K/F224R (m1Venus), and as expected, thanks to restrained basal FRET, Pickles-2.31 containing m1Venus displayed a greater increase in FRET efficiency (80%) than Pickles-2.30 (Supplementary Fig. S1A; Fig. 1B and C). Henceforth, we referred to Pickles-2.31 simply as Pickles and used it throughout the course of this study.

Next, to determine the specificity of Pickles, we examined whether this biosensor would respond to the expression of other kinases. As shown in Fig. 1D, BCR-ABL showed the most significant increase in FRET efficiency among the nonreceptor tyrosine kinases tested, whereas other kinases (expect for c-Abl) failed to do so, consistent with the fact that among Crk family members CrkL and CrkII are major substrates of c-Abl (10). In this regard, it is also noteworthy that the previously reported biosensors based on CrkII (19, 22) displayed similar responsiveness to both BCR-ABL and c-Abl (Supplementary Fig. S1B); we can therefore say that Pickles is a novel biosensor for BCR-ABL with higher specificity and sensitivity than the previous ones. The FRET efficiency of Pickles increased in a BCR-ABL expression–dependent manner, which correlated with the phosphorylation levels of Pickles and endogenous CrkL as determined by immunoblotting (Supplementary Fig. S1C and D). Furthermore, when we introduced Pickles in several leukemia cell lines, K562, KU812, HL60, and U937, the FRET efficiency in BCR-ABL–expressing cells (K562 and KU812) was significantly higher than that in cells without BCR-ABL expression (HL60, U937, and 293F; Supplementary Fig. S1E).

To further confirm that the increase in emission ratio was in fact due to the intramolecular binding of the SH2 domain to phosphorylated Y207, we used three mutants, Pickles-R39V (SH2 domain mutant), Pickles-W160L (NH_2-terminal SH3 domain mutant), and Pickles-Y207F (Y207 mutant). The FRET efficiency of Pickles-R39V and

DOI:10.1158/1078-0432.CCR-10-0548

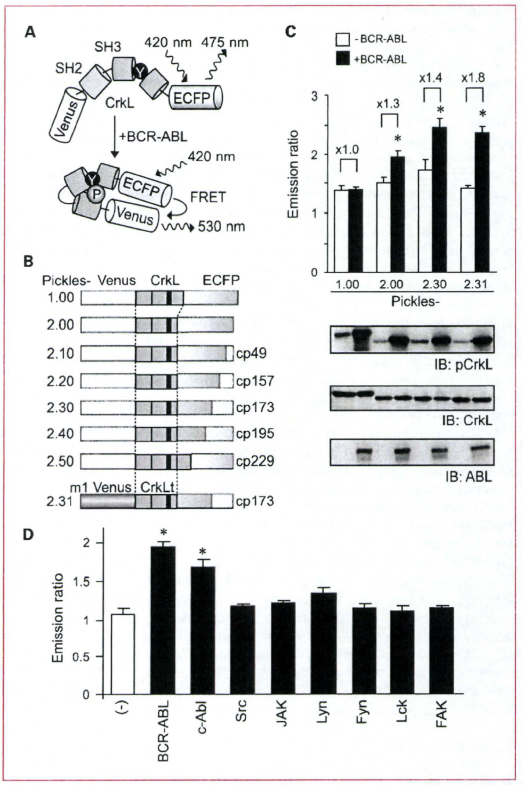

Fig. 1. Development of FRET-based biosensors to monitor CrkL phosphorylation by BCR-ABL. A, schematic representation of nonphosphorylated and phosphorylated Pickles. The sandwiched region consisting of one SH2 and two SH3 domains is from human CrkL. P and Y, a phosphate group and a tyrosine residue corresponding to Y207 of CrkL, respectively. Briefly, Pickles consists of a variant of enhanced yellow fluorescent protein (Venus), CrkL, and ECFP from the NH_2 terminus. Upon Y207 phosphorylation, the SH2 domain binds to this phosphorylated tyrosine, which brings about an increase in the efficiency of FRET from ECFP to Venus. B, domain structures of Pickles-1.00, 2.00, 2.10, 2.20, 2.30, 2.40, 2.50, and 2.31. CrkLt is a COOH terminus–truncated form (1-222 amino acids) of CrkL. Circular permutated (cp) ECFPs have new NH_2 termini: T49, Q157, D173, L195, and I229, as indicated, whereas m1 Venus is a monomeric version of Venus (L222K/F224R). C, emission ratios (FRET/ECFP) and immunoblotting data of Pickles-1.00, 2.00, 2.30, and 2.31 expressed in 293F cells, with or without BCR-ABL. After 24 h, the cells were analyzed with fluorescence spectrometry at an excitation wavelength of 420 nm (top), followed by immunoblotting analysis (bottom). Fluorescence emission is expressed as the mean emission ratio ± SD of pooled data obtained from three separate experiments. D, emission ratios of Pickles-2.31 expressed in 293F cells, with (■) or without (□) tyrosine kinases (bottom). *, $P < 0.05$; values are determined by comparison with control cells (□). Columns, mean obtained from three independent experiments; bars, SD.

Pickles-Y207F failed to increase with BCR-ABL expression, whereas the increase of Pickles-W160L was comparable with that of wild-type Pickles (Supplementary Fig. S1F). As expected, these mutants, except for Pickles-Y207F, were efficiently phosphorylated by BCR-ABL, as measured by immunoblotting (Supplementary Fig. S1G). Because R39 in the SH2 domain is a critical amino acid for phosphotyrosine recognition, presumably Y207 in this case, these experiments reveal that the binding between the SH2 domain and phosphorylated Y207 dictates FRET increase in Pickles. We also confirmed that FRET was indeed the source of this increase in emission ratio through the digestion of Pickles with proteinase K (Supplementary Fig. S1H). Taken together, these results verify that Pickles reports BCR-ABL activity by FRET in response to its SH2-phosphotyrosine binding.

Assessment of the effect of imatinib on BCR-ABL activity using Pickles

Next, we used Pickles to assess the effect of IM on BCR-ABL activity in K562 cells. As expected, FRET efficiency decreased in a dose-dependent manner, the reduction becoming significant at a concentration ≥0.1 μmol/L (Supplementary Fig. S2A; Fig. 2A); however, when we observed the phosphorylation status of endogenous CrkL by immunoblotting and flow cytometry, at least 1 and 0.5 μmol/L IM, respectively, were required to produce a significant difference (Supplementary Fig. S2B and C; Fig. 2B and C).

DOI:10.1158/1078-0432.CCR-10-0548

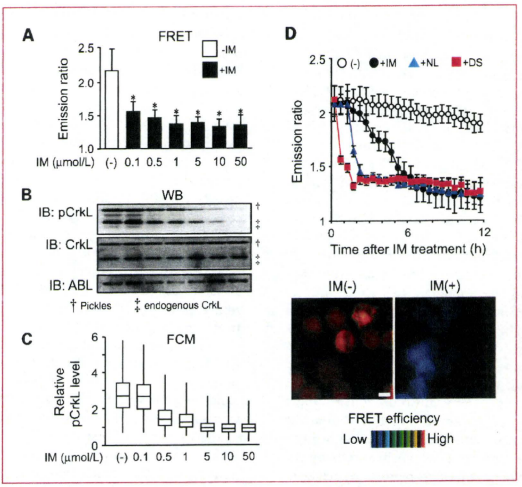

Fig. 2. Evaluation of the efficacy of IM by Pickles. A, K562 cells expressing Pickles were treated with IM (0.1-50 μmol/L) for 24 h as indicated and analyzed by fluorescence spectrometry. Values are expressed as a relative emission ratio in arbitrary units for the mean ± SD of data pooled from three separate experiments. *, $P < 0.05$; values are determined by comparison with control cells (□). B, K562 cells prepared as in A were subjected to immunoblotting. †, Pickles; ‡, endogenous CrkL. Representative results for at least three independent experiments are shown. C, K562 cells were fixed, permeabilized, stained with an anti-phospho CrkL antibody and analyzed by flow cytometry. The phosphorylation level of each cell was displayed in a box-and-whisker plot: lowest and highest boundaries of the box indicate the 25th and 75th percentiles, respectively; the whiskers above and below the box designate the maximum and minimum values, respectively; the solid line within the box represents the median value. D, K562 cells expressing Pickles were subjected to time-lapse fluorescence microscopy. The time course for the emission ratio of K562 in the presence of IM (closed circle), NL (blue triangle), and DS (red square) or in the absence of drugs (open circle) is plotted (top). Bottom, the emission ratio and the intensity of ECFP were used to generate the reconstituted images in the intensity-modulated display (IMD) mode, and photographs before (left) and 24 h after IM treatment (right) are shown. Representative results for at least three separate experiments are shown. See also Supplementary Movie S1.

Moreover, when K562 cells expressing Pickles were subjected to time-lapse dual-emission fluorescence microscopy, they displayed a faithful, time-dependent decrease in FRET efficiency during IM treatment (Fig. 2D, top). After 24 hours, FRET efficiencies were completely inhibited by IM in most cells (see also Supplementary Movie S1; Fig. 2D, bottom). Pickles therefore, being both highly sensitive and practical to use, seems to be a valuable tool to estimate drug efficacy in CML therapy.

Evaluation of the influence of second-generation drugs on BCR-ABL mutants using Pickles

The most serious issue in current IM therapy for CML is the emergence of IM-refractory clones due to various mechanisms—point mutations within the ABL kinase domain being known as the most frequent one (23), stimulating the development of new kinase inhibitors such as NL and DS that are able to override resistance to IM. Pickles could be used successfully to show that the kinetics of these second-generation drugs were faster than that of IM in K562 cells (Fig. 2D, top), in consistence with previous reports (24, 25). To decipher the drug susceptibility of IM-resistant BCR-ABL mutants by Pickles, we prepared constructs for two BCR-ABL mutants, G250E and T315I (26). As expected, these mutants are capable of persistent phosphorylation of CrkL even in the presence of IM, as measured by immunoblotting (Supplementary Fig. S3) as well as by Pickles (Fig. 3A). We could also visualize the drug susceptibility of these mutants in detail: although G250E is sensitive to DS and only high-dose NL, T315I is resistant to all of these drugs (see also Supplementary Fig. S3A and B; Fig. 3A; ref. 26). Interestingly, although the inhibitory effect of NL on the kinase activity of G250E seemed to be dose dependent (Fig. 3A), we also noticed the presence of cells, in which FRET efficiency remained high even after 24 hours of drug treatment. This happened mostly in the cells expressing higher levels of G250E BCR-ABL (Fig. 3C).

Because the inhibitory effect of NL on G250E BCR-ABL remains controversial (26, 27), the above observations

DOI:10.1158/1078-0432.CCR-10-0548

encouraged us to examine whether the expression level of BCR-ABL was in any way related to drug resistance, as has already been proposed (28). Time-lapse analysis revealed a difference in the kinetics of the decrease in FRET efficiency in cells with high and low expression levels of G250E BCR-ABL (Fig. 3B). This difference might be attributed to residual BCR-ABL activity even after NL treatment, which is specifically observed in cells expressing high levels of BCR-ABL at doses of 2 and 20 μmol/L (Fig. 3C). Based on these results, we can state that the expression level of BCR-ABL, particularly that of the G250E mutant, is a determining factor for drug sensitivity. It is noteworthy that even the cells with the high G250E expression became NL sensitive by pretreatment with IM (Supplementary Fig. S3C), which might be accounted for by the synergistic effect between IM and NL as reported (8). These findings further emphasize the indispensable role for this system in determining the most effective drug or drug combinations for BCR-ABL mutants, whichever these may be.

Detection of imatinib resistance by Pickles

In the clinical setting, IM-resistant cells, constituting a very small population of the entire CML cell pool at the initiation of IM therapy, would relapse and supersede due to the elimination of most IM-sensitive cells by the treatment (29, 30). When we tried to reproduce such a situation, Pickles was not useful in portraying the existence of mutant cells; just measuring the average FRET efficiency was insufficient (Supplementary Fig. S4A). To overcome this issue and be able to detect small numbers of drug-resistant cells precisely, we took advantage of the fact that Pickles can be used for single-cell imaging and introduced a threshold value: a dividing line for the FRET value (D-FRET = 2.04), which is defined as the mean emission ratio + (3 × SD) of 293F cells in the absence of BCR-ABL expression (Supplementary Fig. S4B; see also Materials and Methods), into the analyses. We then designated cells having FRET values lower than D-FRET as $FRET^{lo}$ cells, and cells having FRET values higher than D-FRET as $FRET^{hi}$ cells. In theory, >99.7% naïve 293F cells should be $FRET^{lo}$; during our experiments, in over 500 cells analyzed, we never observed any $FRET^{hi}$ naïve 293F cells, irrespective of IM treatment (Supplementary Fig. S4B). In contrast, >50% $FRET^{hi}$ cells can be detected within a native BCR-ABL–expressing cell population, which disappears by drug treatment (Supplementary Fig. S4C and D).

To mimic a more realistic scenario, namely that just a few drug-resistant cells would be dispersed within a large drug-sensitive population, we prepared "mixed" samples consisting of various ratios of native:mutant BCR-ABL–expressing cells and evaluated their drug responses as well as the existence of resistant cells. As shown in Fig. 4A, without IM, box-and-whisker plots displayed comparable patterns of FRET efficiency distributions throughout the mixing ratios. On the other hand, after IM treatment, we could distinguish heterogeneous populations containing

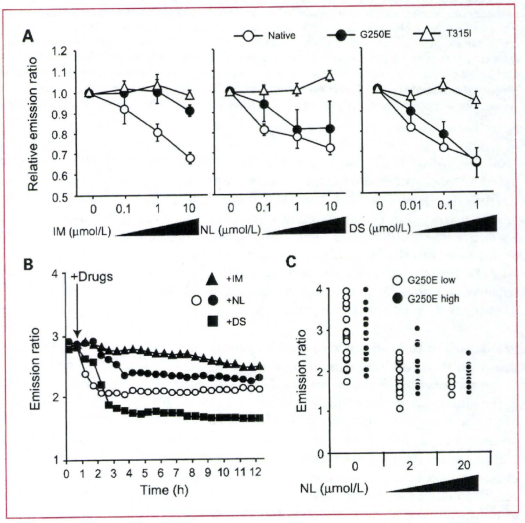

Fig. 3. Measurement of the inhibitory effect of second-generation drugs for BCR-ABL by Pickles. A, 293F cells expressing Pickles and BCR-ABL (native, G250E, or T315I) were treated with the indicated doses of IM, NL, and DS, or left untreated for 24 h, followed by fluorescence spectrometry analysis. Values are expressed as a relative emission ratio in arbitrary units for the mean ± SD of data pooled from three separate experiments. B, 293F cells were transfected with pPickles-2.31 along with 50 ng (○) or 1 μg (▲, ●, ■) of pCMV-BCR-ABL G250E. The cells were then treated with 2 μmol/L IM (▲), 4 μmol/L NL (○, ●) or 0.1 μmol/L DS (■) under a fluorescence microscope. Emission ratios of the cells are plotted. C, 293F cells expressing Pickles were transfected with 50 ng (○, G250E low) or 2 μg (●, G250E high) of an expression vector for BCR-ABL G250E, treated with 2 or 20 μmol/L of NL for 24 h, and analyzed by fluorescence microscopy.

DOI:10.1158/1078-0432.CCR-10-0548

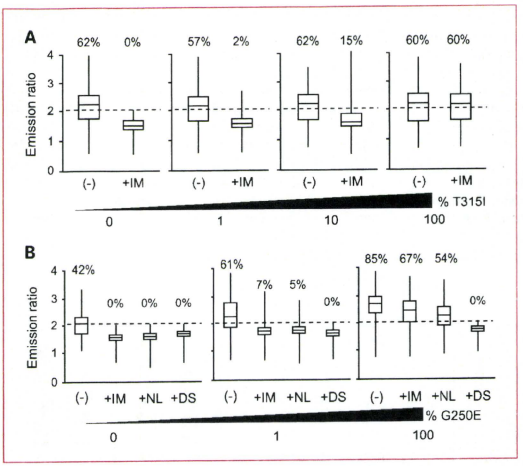

Fig. 4. Detection of IM-resistant populations by Pickles. A and B, Pickles was introduced into 293F cells expressing either native or mutated BCR-ABL (T315I in A; G250E in B). These cells were then mixed at the indicated ratios and treated with 20 μmol/L IM (A), or 20 μmol/L IM, 10 μmol/L NL, and 1 μmol/L DS in B for 24 h. Emission ratios of the cells are plotted in box-and-whisker plots. Dashed line, D-FRET.

drug-resistant cells (even when they represented only 1% of the cell population) from a drug-sensitive homogeneous population by looking at $FRET^{hi}$ cells (Supplementary Fig. S5A; Fig. 4A). In terms of minor drug-resistant cell population detectability, we imagined that a flow cytometric method, which allows for higher throughput analysis might offer advantages over our method, in which the analyzed cell number was limited up to 500 due to manual observation using microscopy. Unexpectedly however, these two methods yielded comparable results, with ~1% of IM-resistant cells within samples being detected (Supplementary Fig. S5A and B; Fig. 4A). Moreover, Pickles is also a useful tool in ascertaining the most effective drug for such minute, resistant cell populations. As shown in Fig. 4B and Supplementary Fig. S5C, we were able to show the sensitivity of small IM- and NL-resistant populations to DS within mixed samples consisting of cells expressing wild-type and G250E BCR-ABL, by the disappearance of $FRET^{hi}$ cells only after DS treatment. Hence, by means of this D-FRET threshold, we succeeded, not only in deciphering drug susceptibility of mutant cells, but also in identifying mutant cells in mixed populations by counting the number of cells remaining above this value.

Using Pickles for drug response evaluation in patients' cells

Next, we applied this technique in primary human CML cells to assess drug efficacy in CML patients. PBMCs and BMCs were first prepared from healthy volunteers or CML patients and then transfected with Pickles. Before FRET analysis, we performed immunofluorescence staining to examine BCR-ABL expression and activity (CrkL phosphorylation) levels, and obtained a surprising result: only a few cells displayed high CrkL phosphorylation along with high BCR-ABL expression (Supplementary Fig. S6A); nevertheless, most cells harbored the Ph, as measured by fluorescence *in situ* hybridization (data not shown). This observation was consistent with a previous report by Keating et al. (31) showing that the expression levels of BCR-ABL transcripts were varied among CML patients. In accordance with the above result, FRET efficiencies of CML cells showed an interspersed distribution, as well as distinct $FRET^{hi}$ cells (coefficient of variation of FRET efficiency = 0.24), whereas those of healthy volunteers exhibited similar low FRET values (coefficient of variation of mean FRET efficiency = 0.11; Supplementary Fig. S6B and C; Fig. 5A, left). Due to the low FRET efficiency exhibited by almost all CML cells, we could obtain significant differences between healthy volunteer and CML patient cells only by using the mean FRET efficiency of the top quartile, but not that of the entire cell population (Fig. 5A, right).

Finally, to show the potential efficacy of our method in patient samples, we show results from our ongoing clinical project, wherein Pickles is introduced into mononuclear cells obtained from CML patients, and the drug efficacy evaluated in PBMC and BMC samples from each individual patient. Until now, we have obtained results that are in concordance with current patient status and are predictive of future outcomes, from 11 patients' samples that have already been analyzed (Table 1), three typical cases (#1-3) of which are displayed here. As shown in Fig. 5B, FRET efficiencies of the top quartile in PBMCs of

DOI:10.1158/1078-0432.CCR-10-0548

cases #1 and #3 were dramatically decreased by IM treatment after 24 hours, and in both cases, $FRET^{hi}$ populations disappeared completely (Fig. 5C, top and bottom). Residual $FRET^{hi}$ populations, however, were observed in case #2 even after IM treatment (Fig. 5C, middle). According to PBMC analysis, therefore, cases #1 and #3 are expected to be sensitive to IM, whereas case #2 is not. In BMCs, the results of cases #1 and #2 were essentially similar to those of PBMCs, i.e., IM sensitive and resistant, respectively [Fig. 5B (right) and D (top and middle)], but for case #3, we obtained paradoxical results. The $FRET^{hi}$ BMC population persisted following IM treatment [Fig. 5B, (right) and D (bottom)], although the $FRET^{hi}$ PBMC population from the same patient decreased in response to IM [Fig. 5B (left) and D (bottom)].

The results above indicated that case #3 possessed IM-refractory tumor cells in the bone marrow but not in the peripheral blood, which encouraged us to carry out a careful follow-up of all three patients during IM treatment. As we anticipated, case #3 achieved complete hematologic response within 2 months, but no CCyR even after 12 months (suboptimal response). Case #1 displayed CCyR after IM administration (optimal response), whereas case #2 could not be successfully managed with IM therapy and underwent bone marrow transplantation following

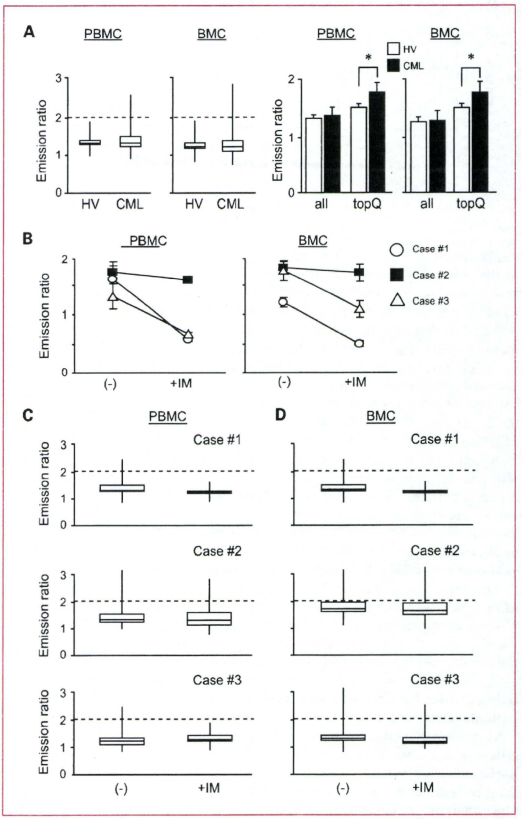

Fig. 5. Evaluation of drug efficacy in primary CML patient cells using Pickles. A, PBMCs and BMCs were purified from peripheral blood or bone marrow of healthy volunteers (HV; $n = 3$) and CML patients (CML; $n = 6$). Emission ratios of cells were plotted in box-and-whisker plots (left). Fluorescence emission is expressed as the mean emission ratio ± SD of pooled data obtained from three separate experiments, for all cells (all) and the top quartile (topQ) of the box-and-whisker plots (right). *, $P < 0.05$; values are determined by comparing healthy volunteers (□) and CML (■) cells. B to D, PBMCs and BMCs were obtained from three CML patients (cases #1-3), transfected with Pickles and incubated in the presence or absence of 2 μmol/L IM. After 24 h, the cells were subjected to dual-emission fluorescence microscopy to determine the FRET efficiency. Mean FRET efficiencies ± SD of the top quartile (B) and box-and-whisker plots (C and D) are shown. Dashed lines (A, C, and D), D-FRET.

DOI:10.1158/1078-0432.CCR-10-0548

Table 1. FRET analysis using clinical samples

Case no.	Age/ gender	Clinical diagnosis	Sample	Assessment by FRET analysis				Clinical IM efficacy/ information
				Before therapy	Months after therapy			
					6	12	18~	
#1	28/M	CML-CP	PBMC	Sensitive	$FRET^{hi}$ (–)			Sensitive-optimal response
			BMC	Sensitive	N.D.	$FRET^{hi}$ (–)		
#2	31/F	Ph-ALL	PBMC	Resistant				Resistance-T315I mutation
			BMC	Resistant				
#3	33/M	CML-CP	PBMC	Sensitive	Resistant			Resistance (200 mg)-suboptimal response*
			BMC	Resistant		$FRET^{hi}$ (±)	$FRET^{hi}$ (–)	Sensitive (400 mg)-N.D.
#4	45/M	CML-CP	BMC				Resistant	Resistance†
#5	21/F	CML-BC	BMC	Resistant				N.D.‡ - received BMT†
#6	59/M	CML-BC	PBMC				Resistant	Resistance†
			BMC				Resistant	
#7	64/M	CML-CP	PBMC	Resistant				Resistance†
#8	73/M	Ph-AML	BMC				Resistant	Resistance§
#9	63/F	CML-CP	PBMC	Resistant				N.D.
#10	65/M	CML-CP	PBMC		$FRET^{hi}$ (–)			Sensitive-complete hematologic remission
#11	42/M	Ph-ALL	BMC	Resistant				N.D.

NOTE: The cells (PBMC or BMC) prepared from patients listed above were subjected to FRET analysis as described in Materials and Methods. Typically obtained results (cases #1-3) are seen in Fig. 5.

Abbreviations: CP, chronic phase; ALL, acute lymphoid leukemia; BC, blast crisis; N.D., not determined; $FRET^{hi}$(–) or $FRET^{hi}$(±), there are no/little $FRET^{hi}$ cells even before IM treatment; BMT, bone marrow transplantation.

*IM dose was increased from 200 to 400 mg/d at 6 mo after initial administration.

†No mutation is detected in *Bcr-abl*.

‡The patient simultaneously received both IM and conventional chemotherapies.

§The patient simultaneously received both IM and interferon therapies.

detection of the multidrug resistant mutation T315I in the *Bcr-abl* gene. In view of the results we are obtaining, we feel confident that following our study using a large patient cohort, this Pickles-based method will be used successfully to provide reliable information about drug sensitivity in CML, both at the time of initial diagnosis and during the course of the disease, as well as to predict potential future recrudescence during/after IM therapy.

Discussion

In the present study, we have developed a FRET-based biosensor, Pickles, which enables the evaluation of BCR-ABL kinase activity in living cells in a quick and efficient manner. To our knowledge, this is the first report in which green fluorescent protein–based FRET technology is applied to such a clinical scene: evaluation of molecular targeted drug efficacy. The discriminatory nature of our method should also be emphasized. Pickles reports the dynamic, functional activity of "live" BCR-ABL protein, which is essentially different from other conventional methods, wherein the information obtained is limited to the amount of BCR-ABL or the static states of CrkL phosphorylation levels after fixation.

The existence of the Ph is the reigning hallmark of disease progression in CML, and its reduction during/after therapy is strikingly associated with the prognoses of CML patients (32). Several approaches, including fluorescence *in situ* hybridization and reverse transcription-PCR, have been introduced for the specific detection of the Ph or its products to show cytogenetic responses (33–35). Given the importance of obtaining major molecular responses (a reduction in BCR-ABL transcript levels of at least 3 log in 12 mo of therapy) to achieve better progression-free survival (36), more sensitive methods such as quantitative reverse transcription-PCR technology have held the limelight in long-term CML management and the monitoring of minimal residual disease in patients with CCyR. More recently, van Dongen and colleagues (37) succeeded in developing a flow cytometric immunobead assay that can

DOI:10.1158/1078-0432.CCR-10-0548

detect a small amount of BCR-ABL protein, irrespective of any mutation. Regrettably however, although these genetic and protein analyses can detect minute BCR-ABL transcripts, translation products, and mutations within them, they provide little useful information for determining an effective second-line therapy for each individual patient, such as, increasing dose of imatinib versus using second-generation tyrosine kinase inhibitors. The fact that our method can evaluate the direct efficacies of drugs at a single cell level, irrespective of the presence or absence of any BCR-ABL mutations, advocates the use of Pickles-based cellular analysis, and we strongly believe that its application, together with quantitative reverse transcription-PCR–based molecular analysis, definitely has the potential to improve the current standard of CML therapy, making it more exact and reliable.

To date, one of the most conventional methods to evaluate IM efficacy is the detection of phosphorylated CrkL by immunoblotting, which is based on the specificity of signaling downstream of BCR-ABL (38, 39). However, this system demands a larger number of cells for drug efficacy evaluation, with a significantly higher order of magnitude than that needed for analysis with Pickles. Moreover, the dynamic range and sensitivity of this probe are, respectively, wider and a 1,000-fold higher than those of Western blotting analysis. Recently, a more sensitive ELISA system based on the detection of phosphorylated CrkL has been proposed (40); however, because cells must be destroyed by the solubilization step required for this test, analysis at the single-cell level is absolutely impossible. Although flow cytometry in combination with intracellular staining of phosphorylated CrkL might be useful with regard to analysis of individual cells (41, 42), another concern associated with these methods remains: selective rapid degradation of BCR-ABL after lysis or permeabilization (43). Therefore, the results obtained by means of the abovementioned techniques will always suffer from the possible underestimation of BCR-ABL activity, which can result in lower sensitivity than expected. In fact, the FRET-based technique described in this study showed similar detectability of small drug-resistant cell populations to that of flow cytometry in spite of its high throughput property (Fig. 4). Given that Pickles can visualize the dynamics of BCR-ABL activity in response to drugs, it apparently exceeds other methods regarding overall detectability.

The abovementioned high performance of Pickles enables the observation of BCR-ABL activity at a single-cell level even if the expression levels or mutant status are variable among cells (Fig. 3). Clinical resistance to IM is attributed to amplification of the *Bcr-abl* gene, clonal evolution, and, most importantly, *Bcr-abl* gene mutations that counter the binding of the target drug. A comprehensive study provides inhibitory profiles of second-generation BCR-ABL kinase inhibitors, such as NL or DS, in term of their activity against the IM-resistant BCR-ABL variants (44). However, variations in the efficacy have also been reported (26, 27), which might be accounted for by the heterogeneity of BCR-ABL activity among CML cells depending on the difference in expression levels, the existence of other additional mutations, and the differentiation status of CML cells. To achieve ideal CML therapy, it is imperative to detect such small aberrant cell populations and identify their character. For instance, O'Hare et al. (26) reported that the G250E mutant is sensitive to NL, whereas Redaelli et al. (27) reported the contrary. Our method disclosed the underlying cause of these paradoxical findings by observation of BCR-ABL activity at a single-cell level (Fig. 3); the sensitivity of BCR-ABL harboring the G250E mutation to NL was totally dependent on its expression level (Fig. 3). This observation apparently provides a guideline for more accurate decision making about NL treatment in the treatment of patients with the G250E mutation.

From another point of view, our method is of significance with regard to the recent emergence of allosteric inhibitors of BCR-ABL. The combined application of this reagent with authentic ATP competitive inhibitors leads to complete disease remissions in an *in vivo* murine CML model (45). Because these new drugs bind to a site far from activation loops, the mutations that affect their sensitivity will be completely different from the ones identified for the authentic drugs, suggesting that to determine the drug efficacy only by sequencing analysis, we must perform an exhaustive search for almost all regions in the *Bcr-abl* gene. Our method will definitely be of great help in such a situation by reporting the direct efficacy of any drugs to any types of BCR-ABL without DNA/RNA sequencing.

Current IM-based CML therapy focuses much attention on CML stem cells, the provenance of leukemic cells, as well as the cells that emerge during relapse (46, 47). Leukemic stem cells are considered to lie concealed within the bone marrow microenvironmental niche in the G_0 phase of the cell cycle (48). In our study, notwithstanding the almost universal presence of the Ph, CML patient cells exhibited a dispersed distribution of BCR-ABL activity, with only 1% to 5% of the total PBMCs being $FRET^{hi}$ (Fig. 5). Although characterization of these $FRET^{hi}$ CML cells and the roles they play in CML pathogenesis is an issue yet to be resolved, CML stem cells, which are reported to express very high levels of functional BCR-ABL (49), might be possible candidates. As yet however, their scarcity ($CD34^+$ $CD38^-$:~1 in 1×10^5 PBMCs or 1×10^3 BMCs; ref. 46) represents an obstacle for such studies. Pickles can be introduced into $CD34^+$ CML cells obtained by bone marrow aspiration with a transfection efficacy comparable with other CML cells (20-30%);[5] thus, it provides an optimistic prospect for investigating the nature of these latent leukemic stem cells. Unfortunately, thus far, no effective treatment to ablate CML stem cells is available, although several next-generation tyrosine kinase inhibitors possess the ability to bind BCR-ABL with known mutations.

The technique described in this study can detect minor drug-resistant populations within heterogeneous cell populations, making it ideal for the evaluation of drug

[5] Unpublished result.

DOI:10.1158/1078-0432.CCR-10-0548

efficacy in CML patients before the initiation of CML therapy, which is of great benefit to both patients and physicians. In fact, our results suggest that the evaluation of BCR-ABL kinase inhibition using Pickles might also be a predictor of long-term molecular responses (Fig. 5), thus allowing for the selection of the best therapeutic approach more accurately than current methods. The Pickles-based method may also be useful in identifying the most suitable treatment for IM-resistant cells irrespective of the refractory mechanism in future; it can be applied to evaluate the effect of newer drugs on CML stem cells and can also be easily incorporated in a high-throughput screening system for the discovery of other tyrosine kinase inhibitors. Hence, following further clinical study, the addition of this novel prognostic molecular response indicator to the present CML therapeutic armamentarium is ultimately envisaged.

Disclosure of Potential Conflicts of Interest

No potential conflicts of interest were disclosed.

Acknowledgments

We thank A. Miyawaki for the Venus cDNA, J. Groffen for the human Crkl. cDNA, D. Baltimore for the BCR-ABL cDNA, H. Hanafusa for the tyrosine kinase cDNAs, T. Hirano for the Janus-activated kinase cDNA, M. Matsuda for the Picchu and human CrkII cDNAs, Novartis Pharma for the IM and NL, Bristol-Myers Squibb for the DS, N. Toyoda for the technical assistance, and members of our laboratory for the helpful discussions.

Grant Support

Supported by Grants-in-Aid for Scientific Research from the Ministry of Education, Culture, Sports, Science and Technology, Japan and the Japan Society for the Promotion of Science, a grant for Research on Publicly Essential Drugs and Medical Devices from the Japan Health Sciences Foundation and a grant from the Yasuda Medical Foundation. T. Mizutani is a Japan Health Sciences Foundation research fellow and S. Darmanin is a JSPS research fellow.

The costs of publication of this article were defrayed in part by the payment of page charges. This article must therefore be hereby marked *advertisement* in accordance with 18 U.S.C. Section 1734 solely to indicate this fact.

Received 03/03/2010; revised 04/21/2010; accepted 05/04/2010; published OnlineFirst 07/29/2010.

References

1. Sawyers C. Targeted cancer therapy. Nature 2004;432:294–7.
2. Kurzrock R, Gutterman JU, Talpaz M. The molecular genetics of Philadelphia chromosome-positive leukemias. N Engl J Med 1988; 319:990–8.
3. Groffen J, Stephenson JR, Heisterkamp N, de Klein A, Bartram CR, Grosveld G. Philadelphia chromosomal breakpoints are clustered within a limited region, bcr, on chromosome 22. Cell 1984;36:93–9.
4. Heisterkamp N, Groffen J, Stephenson JR, et al. Chromosomal localization of human cellular homologues of two viral oncogenes. Nature 1982;299:747–9.
5. Druker BJ, Tamura S, Buchdunger E, et al. Effects of a selective inhibitor of the Abl tyrosine kinase on the growth of Bcr-Abl positive cells. Nat Med 1996;2:561–6.
6. Druker BJ. Translation of the Philadelphia chromosome into therapy for CML. Blood 2008;112:4808–17.
7. Druker BJ, O'Brien SG, Cortes J, Radich J. Chronic myelogenous leukemia. Hematology (Am Soc Hematol Educ Program) 2002; 2002:111–35.
8. Weisberg E, Manley PW, Cowan-Jacob SW, Hochhaus A, Griffin JD. Second generation inhibitors of BCR-ABL for the treatment of imatinib-resistant chronic myeloid leukaemia. Nat Rev Cancer 2007; 7:345–56.
9. Roy L, Guilhot J, Krahnke T, et al. Survival advantage from imatinib compared with the combination interferon-α plus cytarabine in chronic-phase chronic myelogenous leukemia: historical comparison between two phase 3 trials. Blood 2006;108:1478–84.
10. Feller SM. Crk family adaptors-signalling complex formation and biological roles. Oncogene 2001;20:6348–71.
11. Nichols GL, Raines MA, Vera JC, Lacomis L, Tempst P, Golde DW. Identification of CRKL as the constitutively phosphorylated 39-kD tyrosine phosphoprotein in chronic myelogenous leukemia cells. Blood 1994;84:2912–8.
12. Oda T, Heaney C, Hagopian JR, Okuda K, Griffin JD, Druker BJ. Crkl is the major tyrosine-phosphorylated protein in neutrophils from patients with chronic myelogenous leukemia. J Biol Chem 1994;269: 22925–8.
13. ten Hoeve J, Arlinghaus RB, Guo JQ, Heisterkamp N, Groffen J. Tyrosine phosphorylation of CRKL in Philadelphia+ leukemia. Blood 1994;84:1731–6.
14. White D, Saunders V, Lyons AB, et al. *In vitro* sensitivity to imatinib-induced inhibition of ABL kinase activity is predictive of molecular response in patients with *de novo* CML. Blood 2005;106:2520–6.
15. Yamada T, Tsuda M, Ohba Y, Kawaguchi H, Totsuka Y, Shindoh M. PTHrP promotes malignancy of human oral cancer cell downstream of the EGFR signaling. Biochem Biophys Res Commun 2008;368:575–81.
16. Ohba Y, Kurokawa K, Matsuda M. Mechanism of the spatio-temporal regulation of Ras and Rap1. EMBO J 2003;22:859–69.
17. Hamilton A, Elrick L, Myssina S, et al. BCR-ABL activity and its response to drugs can be determined in CD34+ CML stem cells by CrkL phosphorylation status using flow cytometry. Leukemia 2006;20:1035–9.
18. Altman DG, Bland JM. The Normal-Distribution. Br Med J 1995; 310:298.
19. Kurokawa K, Mochizuki N, Ohba Y, Mizuno H, Miyawaki A, Matsuda M. A pair of fluorescent resonance energy transfer-based probes for tyrosine phosphorylation of the Crk II adaptor protein *in vivo*. J Biol Chem 2001;276:31305–10.
20. Nagai T, Ibata K, Park ES, Kubota M, Mikoshiba K, Miyawaki A. A variant of yellow fluorescent protein with fast and efficient maturation for cell-biological applications. Nat Biotechnol 2002;20:87–90.
21. Yoshizaki H, Ohba Y, Kurokawa K, et al. Activity of Rho-family GTPases during cell division as visualized with FRET-based probes. J Cell Biol 2003;162:223–32.
22. Ting AY, Kain KH, Klemke RL, Tsien RY. Genetically encoded fluorescent reporters of protein tyrosine kinase activities in living cells. Proc Natl Acad Sci U S A 2001;98:15003–8.
23. Shah NP, Nicoll JM, Nagar B, et al. Multiple BCR-ABL kinase domain mutations confer polyclonal resistance to the tyrosine kinase inhibitor imatinib (STI571) in chronic phase and blast crisis chronic myeloid leukemia. Cancer Cell 2002;2:117–25.
24. Shah NP, Tran C, Lee FY, Chen P, Norris D, Sawyers CL. Overriding imatinib resistance with a novel ABL kinase inhibitor. Science 2004; 305:399–401.
25. Weisberg E, Manley PW, Breitenstein W, et al. Characterization of AMN107, a selective inhibitor of native and mutant Bcr-Abl. Cancer Cell 2005;7:129–41.
26. O'Hare T, Walters DK, Stoffregen EP, et al. *In vitro* activity of Bcr-Abl inhibitors AMN107 and BMS-354825 against clinically relevant imatinib-resistant Abl kinase domain mutants. Cancer Res 2005;65: 4500–5.
27. Redaelli S, Piazza R, Rostagno R, et al. Activity of bosutinib,

DOI:10.1158/1078-0432.CCR-10-0548

dasatinib, and nilotinib against 18 imatinib-resistant BCR/ABL mutants. J Clin Oncol 2009;27:469–71.
28. Gorre ME, Mohammed M, Ellwood K, et al. Clinical resistance to STI-571 cancer therapy caused by BCR-ABL gene mutation or amplification. Science 2001;293:876–80.
29. Deininger MW, Goldman JM, Melo JV. The molecular biology of chronic myeloid leukemia. Blood 2000;96:3343–56.
30. Jamieson CH, Ailles LE, Dylla SJ, et al. Granulocyte-macrophage progenitors as candidate leukemic stem cells in blast-crisis CML. N Engl J Med 2004;351:657–67.
31. Keating A, Wang XH, Laraya P. Variable transcription of BCR-ABL by Ph+ cells arising from hematopoietic progenitors in chronic myeloid leukemia. Blood 1994;83:1744–9.
32. Sawyers CL. Chronic myeloid leukemia. N Engl J Med 1999;340: 1330–40.
33. Kantarjian H, Sawyers C, Hochhaus A, et al. Hematologic and cytogenetic responses to imatinib mesylate in chronic myelogenous leukemia. N Engl J Med 2002;346:645–52.
34. Tkachuk DC, Westbrook CA, Andreeff M, et al. Detection of bcr-abl fusion in chronic myelogeneous leukemia by *in situ* hybridization. Science 1990;250:559–62.
35. Preudhomme C, Revillion F, Merlat A, et al. Detection of BCR-ABL transcripts in chronic myeloid leukemia (CML) using a "real time" quantitative RT-PCR assay. Leukemia 1999;13:957–64.
36. Hughes TP, Kaeda J, Branford S, et al. Frequency of major molecular responses to imatinib or interferon α plus cytarabine in newly diagnosed chronic myeloid leukemia. N Engl J Med 2003;349: 1423–32.
37. Weerkamp F, Dekking E, Ng YY, et al. Flow cytometric immunobead assay for the detection of BCR-ABL fusion proteins in leukemia patients. Leukemia 2009;23:1106–17.
38. Druker BJ, Talpaz M, Resta DJ, et al. Efficacy and safety of a specific inhibitor of the BCR-ABL tyrosine kinase in chronic myeloid leukemia. N Engl J Med 2001;344:1031–7.
39. White D, Saunders V, Grigg A, et al. Measurement of *in vivo* BCR-ABL kinase inhibition to monitor imatinib-induced target blockade and predict response in chronic myeloid leukemia. J Clin Oncol 2007;25:4445–51.
40. Hamilton A, Alhashimi F, Myssina S, Jorgensen HG, Holyoake TL. Optimization of methods for the detection of BCR-ABL activity in Philadelphia-positive cells. Exp Hematol 2009;37:395–401.
41. Desplat V, Lagarde V, Belloc F, et al. Rapid detection of phosphotyrosine proteins by flow cytometric analysis in Bcr-Abl-positive cells. Cytometry A 2004;62:35–45.
42. Schultheis B, Szydlo R, Mahon FX, Apperley JF, Melo JV. Analysis of total phosphotyrosine levels in CD34+ cells from CML patients to predict the response to imatinib mesylate treatment. Blood 2005; 105:4893–4.
43. Patel H, Marley SB, Gordon MY. Detection in primary chronic myeloid leukaemia cells of p210BCR-ABL1 in complexes with adaptor proteins CBL, CRKL, GRB2. Genes Chromosomes Cancer 2006; 45:1121–9.
44. Azam M, Nardi V, Shakespeare WC, et al. Activity of dual SRC-ABL inhibitors highlights the role of BCR/ABL kinase dynamics in drug resistance. Proc Natl Acad Sci U S A 2006;103:9244–9.
45. Zhang J, Adrian FJ, Jahnke W, et al. Targeting Bcr-Abl by combining allosteric with ATP-binding-site inhibitors. Nature 2010;463:501–6.
46. Bonnet D, Dick JE. Human acute myeloid leukemia is organized as a hierarchy that originates from a primitive hematopoietic cell. Nat Med 1997;3:730–7.
47. Savona M, Talpaz M. Getting to the stem of chronic myeloid leukaemia. Nat Rev Cancer 2008;8:341–50.
48. Dean M, Fojo T, Bates S. Tumour stem cells and drug resistance. Nat Rev Cancer 2005;5:275–84.
49. Copland M, Hamilton A, Elrick LJ, et al. Dasatinib (BMS-354825) targets an earlier progenitor population than imatinib in primary CML but does not eliminate the quiescent fraction. Blood 2006; 107:4532–9.

ORIGINAL RESEARCH ARTICLE

Clin Drug Investig 2010; 30 (4): 1-7
1173-2563/10/0004-0001/$49.95/0

Modified-Irinotecan/Fluorouracil/ Levoleucovorin Therapy as Ambulatory Treatment for Metastatic Colorectal Cancer

Results of Phase I and II Studies

Satoshi Yuuki,[2] *Yoshito Komatsu*,[1] *Nozomu Fuse*,[2] *Takashi Kato*,[2] *Takuto Miyagishima*,[2] *Mineo Kudo*,[2] *Masao Watanabe*,[2] *Miki Tateyama*,[2] *Yasuyuki Kunieda*,[2] *Osamu Wakahama*,[2] *Yu Sakata*[3] and *Masahiro Asaka*[2]

1 Cancer Chemotherapy Division, Hokkaido University Hospital Cancer Center, Sapporo, Japan
2 Department of Gastroenterology, Hokkaido University, Sapporo, Japan
3 Department of Gastroenterology, Misawa City Hospital, Misawa, Japan

Abstract

Background: Combined therapy with irinotecan/fluorouracil/levoleucovorin (calcium levofolinate) [IFL] has lost its position as the standard regimen for metastatic colorectal cancer because its toxicity and effectiveness have become controversial.

Objective: To (i) identify the optimal regimen for IFL therapy in terms of irinotecan dosage, and (ii) determine the maximum tolerated dose and efficacy of the modified-IFL regimen in patients with histologically confirmed advanced colorectal cancer.

Methods: In a phase I study, nine patients with advanced colorectal cancer received IFL treatment modified such that irinotecan was administered every 2 weeks, as opposed to the more toxic once-weekly administration. The study evaluated three escalating dose levels of irinotecan (100, 125 and 150 mg/m^2). Each treatment cycle consisted of irinotecan on days 1 and 15; fluorouracil 600 mg/m^2 on days 1, 8, 15 and 22; and levoleucovorin 250 mg/m^2 on days 1, 8, 15 and 22. Data from the phase I study were used to determine the recommended dose of irinotecan for the phase II study. The latter study evaluated the effectiveness (overall response rate, median time to disease progression and median survival time) and tolerability of this modified-IFL therapy as ambulatory treatment in 22 patients with advanced colorectal cancer.

Results: The dose-limiting toxicity of irinotecan was grade 3 neutropenia, which occurred in three patients at dose level 2 (125 mg/m^2); furthermore, a fourth patient developed grade 4 neutropenia at this dose level. Therefore, 125 mg/m^2 was considered to be the maximum tolerated dose, and the dose of irinotecan for the phase II study was set at 100 mg/m^2. Fourteen patients

achieved partial response using this modified-IFL regimen, and the overall response rate was 63.6% (95% CI 43.5, 83.7). The median time to progression was 197 days (range 111–283 days) and the median survival time was 414 days (95% CI 116, 712). Toxicities were acceptable and manageable.
Conclusions: Modified-IFL therapy is a practical, effective and tolerable option for ambulatory treatment of advanced colorectal cancer.

Background

For the last 40 years, fluorouracil has played a central role in chemotherapy for inoperable or recurrent colorectal cancer, including administration as a continuous infusion, delivery with biochemical modulation therapy to enhance its potency, and other methods of administration. Combined administration of fluorouracil and levoleucovorin (calcium levofolinate) was regarded as the standard therapy until quite recently and may have continued to be the most commonly used regimen worldwide if its survival benefit had been shown to be better. Accordingly, development of more effective drugs and assessment of multiagent regimens are required to achieve progress in the treatment of inoperable or recurrent colorectal cancer.[1-5]

Irinotecan is an anticancer drug developed in Japan that inhibits topoisomerase I, giving this drug a novel mechanism of action. In 1991, Shimada et al.[6] conducted a phase II study of irinotecan monotherapy for previously treated recurrent or advanced colorectal cancer and reported a response rate of 31.3%, demonstrating the effectiveness of this agent. The efficacy of combined therapy with irinotecan, levoleucovorin and fluorouracil (IFL) for previously untreated colorectal cancer has since been confirmed in Europe and the US.[7,8] In 2000, the results of two large-scale, phase II studies were also reported. Saltz et al.[9] performed a comparison of IFL with fluorouracil/levoleucovorin and irinotecan alone, and reported that the three-agent regimen IFL was superior to the other two regimens with respect to response rate and median survival time (MST). Douillard et al.[10] also compared IFL with fluorouracil/levoleucovorin and concluded that the group receiving irinotecan showed a significantly better response. Saltz et al.[9] administered fluorouracil as a bolus and Douillard et al.[10] used the de Gramont regimen (24-hour continuous intravenous infusion). Based on these reports, treatment with IFL became recognized as one of the standard regimens for inoperable colorectal cancer in Europe and the US. However, because levoleucovorin for gastrointestinal cancer was not covered by the Japanese national health scheme until recently, irinotecan/fluorouracil therapy (without levoleucovorin) was studied by the Japan Clinical Oncology Group and its efficacy was reported.[11]

Most of the available data about IFL therapy, including that presented in our previous report,[12] have been obtained from phase I/II clinical studies. FOLFIRI (also a combination of leucovorin/fluorouracil/irinotecan) therapy,[13] in which fluorouracil is administered by continuous infusion, is currently becoming the new standard for inoperable or recurrent colorectal cancer in Europe and the US because the IFL combination developed by Saltz et al.[9] causes severe adverse reactions. However, fluorouracil is administered as a bolus in IFL therapy, which allows outpatient treatment. Accordingly, we performed phase I and II clinical studies to establish a safe regimen for the IFL combination, as well as to determine the maximum tolerated dose (MTD) and the efficacy of this triple therapy in patients with advanced colorectal cancer.

Patients and Methods

Eligibility

The subjects were patients with histologically confirmed inoperable metastatic colorectal cancer or postoperative recurrence, who were managed